A simple method for the analysis of extracellular vesicles enriched for exosomes from human serum by capillary electrophoresis with ultraviolet diode array detection

Oumaima El Ouahabi, Hiba Salim, Roger Pero-Gascon, Fernando Benavente*

Department of Chemical Engineering and Analytical Chemistry, Institute for Research on Nutrition and Food Safety (INSA·UB), University of Barcelona, 08028, Barcelona, Spain

*Corresponding author: fbenavente@ub.edu (F. Benavente, PhD)

Tel: (+34) 934039116, Fax: (+34) 934021233

Keywords: Capillary electrophoresis; dynamic light scattering; exosomes; extracellular vesicles; nanoparticle tracking analysis; polyethylene glycol precipitation.

Abstract

Extracellular vesicles (EVs) are membrane enclosed vesicles (<1 μm), such as exosomes (30-150 nm), involved in cell communication, which have important biological implications. In this study, EV preparations were enriched for exosomes from human serum by polyethylene glycol (PEG) precipitation. Different variables of the PEG precipitation method (i.e. concentration of PEG, filtration and centrifugation of the resuspended pellets) were evaluated by measuring the size of the isolated particles by dynamic light scattering (DLS) and nanoparticle tracking analysis (NTA). In addition, a novel capillary electrophoresis-ultraviolet diode array (CE-UV-DAD) method was developed to obtain characteristic multiwavelength electrophoretic profiles of the EV preparations. Using EV preparations precipitated with 10% m/v of PEG, a background electrolyte (BGE) of 0.1 M Tris and 0.25 M boric acid at pH 7.9 with 0.5% m/v of hydroxypropyl cellulose (HPC) allowed reducing the adsorption of the EVs to the inner wall of the fused silica separation capillary. Sodium dodecyl sulfate (SDS) at 0.1% m/v was also necessary to enhance dispersibility, while homogenizing the charge of the particles to improve the size-dependent separation induced by HPC. Under these optimized conditions, a characteristic electrophoretic multiwavelength profile of the EV preparation and a standard of exosomes was obtained, and separation showed excellent reproducibility and appropriate analysis times. The obtained electrophoretic fingerprints are a simple, effective and complementary tool for the quality control of EV preparations.

1. Introduction

Extracellular vesicles (EVs) comprise a heterogeneous set of membrane enclosed vesicles of different sizes (<1 μm), biological origin and molecular contents, which participate in cell-to-cell communication [1,2]. Nowadays, exosomes (30-150 nm) are the EVs attracting the most interest [2–5]. Exosomes contain lipids, proteins and other small molecules, as well as deoxyribonucleic acid (DNA), messenger ribonucleic acid (mRNA) or microRNA in some cases. They are involved in many physiological and pathological processes, including cancer, inflammation or immune response, and can be found in biological fluids such as blood, urine, sweat and tears. Therefore, exosomes are being targeted as biomarkers, while there is also a growing attention to exploit their potential as drug delivery vehicles [4].

There are many techniques to isolate EV preparations enriched for exosomes [5–10], namely ultracentrifugation, size-exclusion chromatography, ultrafiltration and precipitation with polyethylene glycol (PEG) [7–11]. PEG is a hydrophilic volume-excluding polymer that wraps water molecules and forces the less soluble particles to precipitate [9]. It has been used for purification of viruses [12], and more recently for the selective isolation of exosomes [7–11]. PEG precipitation allows a straightforward, low-cost, reproducible and effective isolation of exosomes from a small volume of sample, without requiring specialized equipment. Several studies have demonstrated the use of PEG of different average molecular weight and concentration for this purpose [8–11]. As with the rest of isolation techniques, the resulting concentrates with PEG are heterogeneous mixtures of exosomes, with other EVs (30-1000 nm, e.g. exomeres, apoptotic bodies, microvesicles, etc) or nanoparticles (protein aggregates, micelles, etc) [2,6]. Further subfractionation and characterization of these EV preparations with current available techniques remains rather challenging [13,14]. However, continuous

advances are being made, such as those focused on the use of flow cytometry [15], microfluidics [16], biosensors [17] or charge detection mass spectrometry [18]. The typical analytical workflows also include dynamic light scattering (DLS) [13,19], nanoparticle tracking analysis (NTA) [13,20], or electron microscopy (EM) [13,21] to provide information about particle size distributions. Among different advantages, the ease of operation makes DLS a widely used technique for particle size analysis at the nanoscale [22,23]. DLS is based on directing a monochromatic laser beam to the particle dispersion and measuring over time the scattered light intensity at a certain angle, which is related to the particle Brownian motion, hence to the translational diffusion coefficient and the particle size [22,23].

Capillary electrophoresis (CE) is a microscale high performance electroseparation technique that in the most basic mode (i.e. capillary zone separation) separates analytes in a capillary tube under the influence of an electric field according to their different charge-to-hydrodynamic radius ratios. CE has been widely demonstrated for the analysis of nanoparticles [24], including gold [25], polymer [26] or quantum dots [27] nanoparticles, liposomes [28], cells, bacteria, viruses and organelles [29–31]. However, the application to intact EVs is very scarce, and only recently M. Piotrowska et al. and M. Morani et al. have described CE methods for the characterization of EV preparations with ultraviolet (UV) and fluorescence detection, respectively [32,33]. In order to expand the application of CE in this field, this study proposes a novel capillary electrophoresis-ultraviolet diode array (CE-UV-DAD) method to obtain characteristic multiwavelength electrophoretic profiles of EV preparations enriched for exosomes from human serum by PEG precipitation. Different variables of the PEG precipitation method are evaluated assisted by DLS size measurements, and the isolated EV preparations allow developing a simple and reproducible CE method using a fused silica

capillary and a near-physiological pH Tris-borate BGE with hydroxypropyl cellulose (HPC) and sodium dodecyl sulfate (SDS). The characteristic multiwavelength electrophoretic fingerprints obtained by CE show potential for the quality control of EV preparations enriched for exosomes.

2. Materials and methods

2.1. Reagents

All reagents were analytical grade or better. PEG with an average molecular weight (MW) of 8,000 Da (PEG8000, 50% m/m) was provided by Fluka (Madrid, Spain). Sodium chloride, potassium chloride, potassium dihydrogen phosphate and HPC with an average MW of 100,000 Da were supplied by Sigma-Aldrich (Madrid, Spain). Sodium hydroxide, sodium hydrogenphosphate and boric acid were purchased from Merck (Darmstadt, Germany). Tris(hydroxymethyl)aminomethane (Tris) and SDS were provided by J. T. Baker (Deventer, Holland) and Promega (Madison, WI, USA), respectively. Water purified with a Milli-Q purification system from Millipore (Molsheim, France) was used for all the experiments.

2.2. Apparatus and procedures

pH measurements were made with a Crison 2002 potentiometer and a Crison electrode 52-03 (Crison Instruments, Barcelona, Spain). Centrifugal filtration at a controlled temperature was carried out in a cooled Rotanta 460 centrifuge (Hettich Zentrifugen, Tuttlingen, Germany). Agitation was performed with a Vortex Genius 3 (Ika®, Staufen, Germany). Incubations were carried out in a TS-100 thermoshaker (Biosan, Riga, Latvian Republic)

2.2.1 Sample preparation

Human blood sample was processed, and research was conducted following standard operation procedures with appropriate approval of the Ethical and Scientific Committees of the University of Barcelona. Venous blood from a healthy donor was collected in an 8.5 mL dry tube with clot activator (BD Vacutainer SST II advance, Becton Dickinson, Madrid, Spain). The blood samples were kept at room temperature for 2 h, and then at 4 °C overnight to improve the clot retraction. The supernatant was separated from the clot with a Pasteur pipette and centrifuged at 1,200 x g for 20 minutes at 4 °C. The serum was aliquoted in 500 µL volumes that were stored in the freezer at -20 ºC when not in use.

The PEG precipitation was performed as described by other authors [8–11], with little adaptations. Under the optimized conditions, PEG was added at a final concentration of 10% m/v to 500 µL of serum. Then, the samples were kept at 4 °C for 2 h followed by low-speed centrifugation at 3,000 x g for 10 min at 4 °C. The supernatant was discarded, and the pellet was washed three times with 50 µL of phosphate buffer saline (PBS, 10 mM Na_2HPO_4, 2 mM KH_2PO_4, 137 mM NaCl and 2.7 mM KCl, pH 7.3). In each wash, the sample was vortexed and then centrifuged at 3,000 x g for 3 min at 4 °C to separate the pellet. The final pellet was resuspended in 125 µL of PBS.

Purified lyophilized exosomes isolated through a combination of ultracentrifugation and microfiltration procedures from serum of healthy donors were provided by HansaBioMed Life Sciences (Tallinn, Estonia). They were reconstituted in PBS to obtain a final concentration of 1 µg/mL.

The EV preparations and the standard exosomes were analyzed immediately, or they were kept in the refrigerator at 4 ºC for no longer than 48 h before the analysis.

2.2.2. DLS

The DLS measurements were done with a Zetasizer Nano ZS apparatus with a low-volume quartz batch cuvette ZEN2112 (Malvern Instruments, Malvern, UK). For appropriate measurements, the EV preparations were diluted 1:10 v/v in PBS before the analyses. PBS was filtered before the dilution (0.2 µm nylon filters). The diluted EV preparations were analyzed without further processing, as well as after filtration (0.2 µm nylon filters) or centrifugation (1,250 x g for 3 min at 25 ºC). The clean cuvette was washed 3 times with water and acetone and then dried with air, before checking that no particles were detected in filtered PBS and 1% m/v of PEG in PBS (i.e. the measurement indicated error because counts were insufficient for reliable results). Seventy five µL of blank solution or sample were used for the analyses. The backscatter employed was with a detection system at 173°. The equilibration time was 5 s and the scan duration was 70 s. Measurements were performed in triplicate at 25 ºC, setting the refractive index at 1.37 for the nanoparticles and 1.33 for water as a dispersant, following the manufacturer suggestions. The viscosity was set at 0.00089 mPa s.

2.2.3 NTA

Size distribution and particle concentration were measured by NTA with a NanoSight NS300 system (Malvern Instruments). In order to match the optimal concentration range of the instrument and track individual nanoparticles, the EV preparations were diluted 1:500 v/v in PBS before the analyses. PBS was filtered before the dilution (0.2 µm nylon filters).

2.2.4. CE-UV-DAD

CE-UV-DAD experiments were conducted in a 7100 CE instrument (Agilent Technologies, Waldbronn, Germany). Separations were performed at 25 °C in 55 cm total length (L_T) × 46.5 cm detector length (L_D) x 75 µm internal diameter (i.d.) × 365 µm outer diameter (o.d.) fused silica capillaries (Polymicro Technologies, Phoenix, AZ, USA). All solutions were passed through 0.2 µm nylon filters (Macherey-Nagel, Düren, Germany) and stored in glass bottles at 4 ºC. Before the analyses, the BGE was degassed by sonication. All capillary flushes were performed at high pressure (930 mbar). Under the optimized conditions, the background electrolyte (BGE) was a 0.1 M Tris and 0.25 M boric acid solution (pH 7.9) with 0.5% m/v of HPC and 0.1% m/v of SDS. New fused silica capillaries were flushed with water (20 min), 1 M NaOH (20 min), water (20 min) and BGE (20 min). The capillary was finally equilibrated by applying +25 kV (normal polarity, cathode in the outlet) for 30 min. EV preparations were injected without further processing at 50 mbar for 10 s. The autosampler was kept at 25 °C using an external water bath (Minichiller 300, Peter Huber Kältemaschinenbau AG, Offenburg, Germany). Between runs, capillaries were conditioned by flushing with water (2 min), 1 M NaOH (2 min), water (2 min) and BGE (2 min). The UV-spectra were recorded scanning from 190 to 300 nm. Data acquisition was performed with OpenLab CDS ChemStation Edition C.01.07 SR3 software (Agilent Technologies).

3. Results and discussion

3.1 EV preparation by PEG precipitation

PEG precipitation was the method selected for the isolation of the EV preparations enriched for exosomes from serum samples, because of the simplicity, the possibility of avoiding the use of expensive kits, and the effectivity and reproducibility demonstrated in previous studies. Several authors have demonstrated that the

performance of PEG precipitation to isolate exosomes depends on the average molecular weight of PEG, the concentration upon mixing with the sample, the temperature and exosome concentration [8–11]. In this study, following the recommendations of Vlassov et al. for PEG8000 [8], PEG concentrations of 5, 7.5 and 10% m/v were investigated for precipitation at 4 °C and 2 h incubation. Using these conditions, as can be observed in Figure 1, the expected precipitated pellet for the EV preparations was observed in all cases. Furthermore, even by naked eye, it could be seen that the pellet amount slightly increased with PEG concentration, being apparently the highest with 10% m/v of PEG (Figure 1C).

3.2 DLS

DLS was used to measure the size distribution of the particles of the EV preparations that were isolated from serum using different concentrations of PEG. As the resuspended pellets in PBS were turbid and not suitable for DLS measurements, the samples were diluted 1:10 v/v with PBS before the analysis. The polydispersity index (PDI) measured for the diluted samples were in all cases around 0.4 (Table 1), a value in the recommended range for appropriate size measurements by DLS (i.e. <0.7) [22,23]. As can be observed in the graph of size-distribution by intensity (Figure 2A), nanoparticles with a similar size distribution were detected in the EV preparations with all the PEG concentrations. Considering the sample with 10% m/v PEG, the most intense peak corresponded to particles with sizes ranging from approximately 128 to 356 nm, and an average size of 242 nm (Table 1). Meanwhile, the less intense peak represented particles ranging approximately from 34 to 66 nm, with an average size of 50 nm (Table 1). The measured sizes were slightly different than the typically reported sizes for exosomes (i.e. 30-150 nm) and were far from the upper size limits expected for

other EVs (1000 nm) [2,18]. Therefore, it was confirmed the selectivity of PEG precipitation to isolate EVs in a narrow size range, which includes exosomes. However, PEG would induce clumping or aggregation of the largest exosomes and EVs (i.e. >66 nm), and because of this the size distribution was shifted to higher values than expected. Weng et al. have already shown that exosomes isolated by PEG precipitation appear by EM wrapped by a silky PEG film, forming aggregates [9]. The graph of size distribution by intensity (Figure 2A) was converted to the graph of size distribution by volume (Figure 2B) to investigate the relative proportion of the different particle sizes in the samples [22]. The results obtained were again very similar with the different concentrations of PEG, but now only a single intense peak could be clearly observed. This was because small particles (average size of 50 nm, with 10% m/v PEG, Table 1) were more abundant but scattered much less light than large particles (average size of 242 nm, with 10% m/v PEG, Table 1). A similar conclusion could be obtained from the graph of size distribution by number that indicates the relative number of particles with a certain size in the samples (Figure S-1) [22].

The diluted EV preparations were also analyzed after filtration or centrifugation to see the effect on the particle size distribution. Figure 2C shows the graph of size distribution by intensity for the diluted EV preparations with a 10% m/v PEG, and after filtration or centrifugation. As can be observed, the particle size distribution was shifted to lower values only for the filtered samples, suggesting that large particles were eliminated. Furthermore, the filtered sample was less polydisperse because the measured PDI value decreased until 0.3 (Table 1). The sizes measured for the particles of the filtered samples were ranging from approximately 67 to 171 nm, and an average size of 119 nm (Table 1), and from 20 nm to 34 nm, and an average size of 27 nm (Table 1). These sizes were within the size range expected for exosomes (i.e. 30-150

nm) and would indicate the necessity of filtering the samples to further enrich the EV preparations for exosomes. Weng et al. also reported that when exosomes isolated by PEG precipitation were greatly diluted to perform appropriate NTA measurements, PEG concentration was insufficient to induce aggregation and the size distribution presented a narrow peak with a maximum at 100 nm [9]. Similarly, in our case, the measured average particle size by NTA for the EV preparations with a 10% m/v PEG was 120 nm when the sample was diluted 1:500 v/v with PBS before the analysis (Figure S-2). In order to evaluate if filtration had a negative impact on the particle concentration, the derived count rate (DCR) was studied for the isolated EV preparations with the different PEG concentrations and sample conditions. DCR is the number of photons detected per second divided by the attenuation factor given by the DLS instrument software [34]. Therefore, in general, the greater the DCR value the higher the particle concentration (if particle size distributions are similar). As can be observed in Table 2, the greatest DCR parameter values were obtained with the different PEG concentrations for the "diluted" and "diluted+centrifuged" samples, confirming that centrifugation was not significantly altering the particle size distribution of the "diluted" sample. The use of a 5% m/v of PEG promoted a great decrease on particle concentration, compared to 7.5 and 10% m/v of PEG, confirming that EVs precipitation was less efficient at the lowest PEG concentration, as previously observed by naked eye (Figure 1). As expected, filtration promoted in all cases a great decrease on particle concentration, due to elimination of large particles. Therefore, the elimination of the large EVs aggregates with PEG was at a cost of decreasing the total EVs recoveries. As the particle concentration was slightly higher for the EV preparation isolated with a 10% than with a 7.5% m/v of PEG without further processing (compare the DCR values of Table 2 for both "diluted" EV

preparations), undiluted EV preparations with a 10% m/v of PEG were used to develop the novel CE-UV-DAD fingerprinting method.

3.3 CE-UV-DAD

The EV preparation was analyzed first using a BGE of 0.1 M Tris and 0.25 M boric acid (pH 7.9). Tris-borate BGEs at near-physiological pH values have been traditionally used in CE analysis of oligonucleotides, proteins and more recently nanoparticles because of the excellent performance [27,30,35–37]. At these pH values, EVs were less prone to aggregation and they had a total negative charge that was supposed to prevent adsorption on the inner wall of the bare fused silica capillary [38]. However, under these conditions, results were not reproducible (Figure S-3). Furthermore, the electrophoretic profiles did not correspond to the expected profiles for a mixture of nanoparticles with a relatively broad size distribution. These poor results were suggesting the strong adsorption of the EVs on the inner capillary wall of the bare fused silica capillary. Despite the total negative charge of EVs at the separation pH value, it should not be forgotten that some EVs, as exosomes, are amphoteric and present basic proteins on the surface, which would promote this adsorption.

In order to reduce the adsorption of the EVs to the ionized silanol groups of the inner capillary wall, addition of small concentrations of the neutral linear polymer HPC (0.3, 0.5 and 0.8% m/v) to the BGE was investigated [36,37]. As can be seen in Figure 3, the results obtained were very distinct between the different concentrations of HPC. A very wide band was migrating after the EOF for the concentration of 0.3% m/v HPC (Figure 3A). By increasing the HPC concentration to 0.5% m/v results improved and two bands with a smaller width were clearly visible at shorter migration times (Figure 3B). These bands were dotted with very narrow peaks (i.e. spikes), which were

randomly distributed when replicate analyses were done (Figure 4A). Therefore, they were probably due to air bubbles and/or large aggregates of EVs trapped and arriving to the detector in the heterogeneous mixture of EVs with different sizes. This spiking phenomenon was also described before by other authors in CE analysis of other nanoparticles, including EVs [25,29,30,32,33]. The two bands were less clearly visible with a 0.8% m/v of HPC because the number and widths of the spikes greatly increased (Figure 3C), as a consequence of the increase on BGE viscosity and/or HPC entanglement [36]. Therefore, a concentration of 0.5% m/v of HPC was used for the rest of experiments. At this point, it is worth highlighting, that at the slightly basic pH value of the BGE (7.9), the small amount of HPC added in the BGE was not enough to significantly reduce the EOF (compare the EOF migration time in Figures S-2 and Figure 3B), as previously observed by other authors [39]. Consequently, while preventing the adsorption on the capillary, the EOF remained high enough to promote migration of the negatively charged EVs to the detector. Regarding the separation mechanism, at a 0.5% m/v of HPC, an HPC of average MW of 100,000 Da would be under the entanglement threshold, and separation would occur under a transient entanglement coupling size-dependent mechanism between the EVs and the polymer chains [36].

To further improve reproducibility, 0.1% m/v of SDS was added to the BGE with 0.5% m/v of HPC. The role of the anionic surfactant at a concentration below the critical micelle concentration (i.e. CMC 8.2 $mmol \cdot L^{-1}$ or 0.24% m/v in aqueous solutions) was to improve the dispersion of the EVs, while homogenizing the total negative charge by complexation with the protonated basic groups of the amphoteric EVs to improve the size-dependent separation. Furthermore, it has also been described the positive effect of SDS on preventing protein adsorption on the inner capillary walls

[37]. Figure 4B shows the electropherograms for ten replicate analyses of an EV preparation (replicates 1st, 5th and 10th) and for the blank samples under these conditions. As can be observed, the EV preparation was detected now as peaks and bands after the EOF and total analysis time was reduced to less than 30 min, spikes were not present, and the electrophoretic profile was repeatable for the different replicates (i.e. the relative standard deviation in percentage, %RSD (n=10) of migration time (in the apex) and peak area for the indicated region in Figure 4B were 1.2% and 5.1%, respectively). A careful analysis of the UV spectra through the obtained multiwavelength electrophoretic profile of the EV preparations allowed detecting three different characteristic regions with a specific UV spectrum (labelled as I, II and III in Figure 5A). Figure 5C shows the characteristic UV spectra for these three regions, which would have increasing particle sizes. As can be observed in the UV spectra of Figure 5C, some differences could be observed in the scanned range, suggesting that distinct types of EVs were detected, being the most abundant those migrating in the region labelled as II in Figure 5A. Even accepting the proposed size-based separation mechanism, at this moment, it is difficult to correlate the information about particle size obtained by DLS and the electrophoretic profiles obtained by CE. This is because the composition of the BGE and the high electrical field could definitively alter the particle size distribution by promoting disruption of the EVs aggregates detected by DLS. A standard of exosomes was analyzed (Figure 5B) to confirm that they would be migrating in the region corresponding to the most abundant EVs (region II, Figure 5A). As can be observed in Figure 5C, the exosomes were also showing a differential UV spectrum compared to those obtained for the EV preparation characteristic region II, where different types of EVs were comigrating (Figure 5C).

Regarding the electrophoretic profiles with independent EV preparations, reproducibility was good for EV preparations isolated and analyzed in different days (i.e. %RSD (n=3) of migration time and peak area for region II in Figure S-4 were 2.9% and 5.5%, respectively). CE analyses were also repeated after storing the samples in the refrigerator (4 °C) for four days and the electrophoretic profiles changed. Therefore, as the lifetime of the samples seemed to be quite short, analysis of the EV preparations by DLS and CE-UV within the first 48 h after the isolation with PEG is recommended. Globally, the results demonstrated the good performance of PEG precipitation for isolation of EV preparations from serum samples and of the developed CE method to perform a simple, effective and complementary quality control. Compared to the CE methods recently described for the analysis of EVs [32,33], the developed CE method generated similar electrophoretic profiles for the EVs and the standard of exosomes. However, demonstrated improved efficacy for prevention of the spiking phenomenon while obtaining highly reproducible separations of extremely complex EV preparations without needing expensive commercial or hard to prepare permanently coated capillaries. This was probably mainly due to the use of a wider i.d. capillary (75 µm instead of 50 µm), as well as to the presence of HPC and SDS in the near-physiological pH Tris-borate BGE. With regard to sensitivity, at the moment, the use of fluorescence detection allows better limits of detection than UV detection, as described by M. Morani et al. [33]. However, it requires off-line derivatization of the isolated EVs. A more versatile and straightforward alternative would be applying on-line preconcentration approaches, as explored to a certain extent with isotachophoresis by M. Piotrowska et al. [32]. However, further research is needed to efficiently increase the modest preconcentration factors obtained so far and expand the applicability of CE in the typical workflows applied in characterization of purified EVs, including exosomes.

4. Conclusions

Precipitation with a 10% m/v of PEG8000 was successfully applied for the isolation of EV preparations enriched for exosomes from human serum samples. DLS demonstrated that nanoparticles within a very narrow size range that includes the exosomes, were present in the EV preparations. The most abundant particles had an average size of 50 nm, but 242 nm particles were also detected, suggesting that PEG would induce aggregation. Filtration allowed further enriching the EV preparations for exosomes, but at a cost of decreasing the recoveries. Using the isolated EV preparations, a novel CE-UV-DAD method was developed to obtain characteristic multiwavelength electrophoretic profiles. A BGE of 0.1 M Tris and 0.25 M boric acid (pH 7.9) with 0.5% m/v HPC and 0.1% m/v of SDS was optimized to obtain reproducible and rapid separations of the EV preparations and standard exosomes. The CE-UV-DAD fingerprinting method may find applicability as a complementary tool for the simple and effective quality control of EV preparations enriched for exosomes. However, further research is necessary to identify the different components detected in the electrophoretic fingerprints and enhance sensitivity to analyze low concentration purified EV samples. The method may be adapted to the direct, selective and sensitive detection and characterization of specific EVs at the intact level, especially exosomes.

Acknowledgements

This study was supported by the Spanish Ministry of Economy and Competitiveness (RTI2018-097411-B-I00) and the Cathedra UB Rector Francisco Buscarons Úbeda

(Forensic Chemistry and Chemical Engineering). Hiba Salim acknowledges the UB Solidarity Foundation and the Global Platform for Syrian Students for the scholarships at the University of Barcelona. The authors thank Jose Amable Bernabé from the Biomaterial Processing and Nanostructuring Unit of the ICTS "NANBIOSIS" (CIBER-BBN, ICMAB-CSIC) for performing the NTA measurements.

The authors declare no conflicts of interest.

References

[1] M. Shang, J.S. Ji, C. Song, B.J. Gao, J.G. Jin, W.P. Kuo, H. Kan, Extracellular vesicles: A brief overview and its role in precision medicine, in: W.P. Kuo, S. Jia (Eds.), Extracellular Vesicles. Methods in Molecular Biology, 1st ed., Springer Science+Business Media, 2017: pp. 1–14. doi:10.1007/978-1-4939-7253-1_1.

[2] G. Van Niel, G. D'Angelo, G. Raposo, Shedding light on the cell biology of extracellular vesicles, Nat. Rev. Mol. Cell Biol. 19 (2018) 213–228. doi:10.1038/nrm.2017.125.

[3] M. Colombo, G. Raposo, C. Théry, Biogenesis, secretion, and intercellular interactions of exosomes and other extracellular vesicles, Annu. Rev. Cell Dev. Biol. 30 (2014) 255–289. doi:10.1146/annurev-cellbio-101512-122326.

[4] Y. Zhang, Y. Liu, H. Liu, W.H. Tang, Exosomes: Biogenesis, biologic function and clinical potential, Cell Biosci. 9 (2019) 19. doi:10.1186/s13578-019-0282-2.

[5] K. Boriachek, M.N. Islam, A. Möller, C. Salomon, N.T. Nguyen, M.S.A. Hossain, Y. Yamauchi, M.J.A. Shiddiky, Biological functions and current advances in isolation and detection strategies for exosome nanovesicles, Small. 14 (2018) 1–21. doi:10.1002/smll.201702153.

[6] P. Li, M. Kaslan, S.H. Lee, J. Yao, Z. Gao, Progress in exosome isolation techniques, Theranostics. 7 (2017) 789–804. doi:10.7150/thno.18133.

[7] T.J. Antes, K. Kwei, F. Wu, Methods for microvesicle isolation and selective removal, US 9,005,888 B2, 2015.

[8] A. Vlassov, M. Li, E. Zeringer, R. Conrad, Methods and compositions for exosome isolation, US8,901,284 B2, 2014.

[9] Y. Weng, Z. Sui, Y. Shan, Y. Hu, Y. Chen, L. Zhang, Y. Zhang, Effective isolation of exosomes with polyethylene glycol from cell culture supernatant for in-depth proteome profiling, Analyst. 141 (2016) 4640–4646. doi:10.1039/c6an00892e.

[10] A.K. Ludwig, K. De Miroschedji, T.R. Doeppner, V. Börger, J. Ruesing, V. Rebmann, S. Durst, S. Jansen, M. Bremer, E. Behrmann, B.B. Singer, H. Jastrow, J.D. Kuhlmann, F. El Magraoui, H.E. Meyer, D.M. Hermann, B. Opalka, S. Raunser, M. Epple, P.A. Horn, B. Giebel, Precipitation with polyethylene glycol followed by washing and pelleting by ultracentrifugation enriches extracellular vesicles from tissue culture supernatants in small and large scales, J. Extracell. Vesicles. 7 (2018) 1528109. doi:10.1080/20013078.2018.1528109.

[11] M.A. Rider, S.N. Hurwitz, D.G. Meckes, ExtraPEG: A polyethylene glycol-based method for enrichment of extracellular vesicles, Sci. Rep. 6 (2016) 1–14. doi:10.1038/srep23978.

[12] G. D. Lewis, T. G. Metcalf, Polyethylene glycol precipitation for recovery of pathogenic viruses, including hepatitis a virus and human rotavirus, from oyster, water, and sediment samples, Appl. Environ. Microbiol. 54 (1988) 1983–1988. doi:10.1128/AEM.54.8.1983-1988.1988.

[13] R. Szatanek, M. Baj-Krzyworzeka, J. Zimoch, M. Lekka, M. Siedlar, J. Baran,

The methods of choice for extracellular vesicles (EVs) characterization, Int. J. Mol. Sci. 18 (2017) 1153. doi:10.3390/ijms18061153.

[14] C. Théry, K.W. Witwer, E. Aikawa, M.J. Alcaraz, J.D. Anderson, R. Andriantsitohaina, A. Antoniou, T. Arab, F. Archer, G.K. Atkin-Smith, D.C. Ayre, J.-M. Bach, D. Bachurski, H. Baharvand, L. Balaj, S. Baldacchino, N.N. Bauer, A.A. Baxter, M. Bebawy, C. Beckham, A. Bedina Zavec, A. Benmoussa, A.C. Berardi, P. Bergese, E. Bielska, C. Blenkiron, S. Bobis-Wozowicz, E. Boilard, W. Boireau, A. Bongiovanni, F.E. Borràs, S. Bosch, C.M. Boulanger, X. Breakefield, A.M. Breglio, M.Á. Brennan, D.R. Brigstock, A. Brisson, M.L. Broekman, J.F. Bromberg, P. Bryl-Górecka, S. Buch, A.H. Buck, D. Burger, S. Busatto, D. Buschmann, B. Bussolati, E.I. Buzás, J.B. Byrd, G. Camussi, D.R. Carter, S. Caruso, L.W. Chamley, Y.-T. Chang, C. Chen, S. Chen, L. Cheng, A.R. Chin, A. Clayton, S.P. Clerici, A. Cocks, E. Cocucci, R.J. Coffey, A. Cordeiro-da-Silva, Y. Couch, F.A. Coumans, B. Coyle, R. Crescitelli, M.F. Criado, C. D'Souza-Schorey, S. Das, A. Datta Chaudhuri, P. de Candia, E.F. De Santana, O. De Wever, H.A. del Portillo, T. Demaret, S. Deville, A. Devitt, B. Dhondt, D. Di Vizio, L.C. Dieterich, V. Dolo, A.P. Dominguez Rubio, M. Dominici, M.R. Dourado, T.A. Driedonks, F. V Duarte, H.M. Duncan, R.M. Eichenberger, K. Ekström, S. EL Andaloussi, C. Elie-Caille, U. Erdbrügger, J.M. Falcón-Pérez, F. Fatima, J.E. Fish, M. Flores-Bellver, A. Försönits, A. Frelet-Barrand, F. Fricke, G. Fuhrmann, S. Gabrielsson, A. Gámez-Valero, C. Gardiner, K. Gärtner, R. Gaudin, Y.S. Gho, B. Giebel, C. Gilbert, M. Gimona, I. Giusti, D.C. Goberdhan, A. Görgens, S.M. Gorski, D.W. Greening, J.C. Gross, A. Gualerzi, G.N. Gupta, D. Gustafson, A. Handberg, R.A. Haraszti, P. Harrison, H. Hegyesi, A. Hendrix, A.F. Hill, F.H. Hochberg, K.F. Hoffmann, B. Holder, H.

Holthofer, B. Hosseinkhani, G. Hu, Y. Huang, V. Huber, S. Hunt, A.G.-E. Ibrahim, T. Ikezu, J.M. Inal, M. Isin, A. Ivanova, H.K. Jackson, S. Jacobsen, S.M. Jay, M. Jayachandran, G. Jenster, L. Jiang, S.M. Johnson, J.C. Jones, A. Jong, T. Jovanovic-Talisman, S. Jung, R. Kalluri, S. Kano, S. Kaur, Y. Kawamura, E.T. Keller, D. Khamari, E. Khomyakova, A. Khvorova, P. Kierulf, K.P. Kim, T. Kislinger, M. Klingeborn, D.J. Klinke, M. Kornek, M.M. Kosanović, Á.F. Kovács, E.-M. Krämer-Albers, S. Krasemann, M. Krause, I. V Kurochkin, G.D. Kusuma, S. Kuypers, S. Laitinen, S.M. Langevin, L.R. Languino, J. Lannigan, C. Lässer, L.C. Laurent, G. Lavieu, E. Lázaro-Ibáñez, S. Le Lay, M.-S. Lee, Y.X.F. Lee, D.S. Lemos, M. Lenassi, A. Leszczynska, I.T. Li, K. Liao, S.F. Libregts, E. Ligeti, R. Lim, S.K. Lim, A. Linē, K. Linnemannstöns, A. Llorente, C.A. Lombard, M.J. Lorenowicz, Á.M. Lörincz, J. Lötvall, J. Lovett, M.C. Lowry, X. Loyer, Q. Lu, B. Lukomska, T.R. Lunavat, S.L. Maas, H. Malhi, A. Marcilla, J. Mariani, J. Mariscal, E.S. Martens-Uzunova, L. Martin-Jaular, M.C. Martinez, V.R. Martins, M. Mathieu, S. Mathivanan, M. Maugeri, L.K. McGinnis, M.J. McVey, D.G. Meckes, K.L. Meehan, I. Mertens, V.R. Minciacchi, A. Möller, M. Møller Jørgensen, A. Morales-Kastresana, J. Morhayim, F. Mullier, M. Muraca, L. Musante, V. Mussack, D.C. Muth, K.H. Myburgh, T. Najrana, M. Nawaz, I. Nazarenko, P. Nejsum, C. Neri, T. Neri, R. Nieuwland, L. Nimrichter, J.P. Nolan, E.N. Nolte-’t Hoen, N. Noren Hooten, L. O’Driscoll, T. O’Grady, A. O’Loghlen, T. Ochiya, M. Olivier, A. Ortiz, L.A. Ortiz, X. Osteikoetxea, O. Østergaard, M. Ostrowski, J. Park, D.M. Pegtel, H. Peinado, F. Perut, M.W. Pfaffl, D.G. Phinney, B.C. Pieters, R.C. Pink, D.S. Pisetsky, E. Pogge von Strandmann, I. Polakovicova, I.K. Poon, B.H. Powell, I. Prada, L. Pulliam, P. Quesenberry, A. Radeghieri, R.L. Raffai, S. Raimondo, J.

Rak, M.I. Ramirez, G. Raposo, M.S. Rayyan, N. Regev-Rudzki, F.L. Ricklefs, P.D. Robbins, D.D. Roberts, S.C. Rodrigues, E. Rohde, S. Rome, K.M. Rouschop, A. Rughetti, A.E. Russell, P. Saá, S. Sahoo, E. Salas-Huenuleo, C. Sánchez, J.A. Saugstad, M.J. Saul, R.M. Schiffelers, R. Schneider, T.H. Schøyen, A. Scott, E. Shahaj, S. Sharma, O. Shatnyeva, F. Shekari, G.V. Shelke, A.K. Shetty, K. Shiba, P.R.-M. Siljander, A.M. Silva, A. Skowronek, O.L. Snyder, R.P. Soares, B.W. Sódar, C. Soekmadji, J. Sotillo, P.D. Stahl, W. Stoorvogel, S.L. Stott, E.F. Strasser, S. Swift, H. Tahara, M. Tewari, K. Timms, S. Tiwari, R. Tixeira, M. Tkach, W.S. Toh, R. Tomasini, A.C. Torrecilhas, J.P. Tosar, V. Toxavidis, L. Urbanelli, P. Vader, B.W. van Balkom, S.G. van der Grein, J. Van Deun, M.J. van Herwijnen, K. Van Keuren-Jensen, G. van Niel, M.E. van Royen, A.J. van Wijnen, M.H. Vasconcelos, I.J. Vechetti, T.D. Veit, L.J. Vella, É. Velot, F.J. Verweij, B. Vestad, J.L. Viñas, T. Visnovitz, K. V Vukman, J. Wahlgren, D.C. Watson, M.H. Wauben, A. Weaver, J.P. Webber, V. Weber, A.M. Wehman, D.J. Weiss, J.A. Welsh, S. Wendt, A.M. Wheelock, Z. Wiener, L. Witte, J. Wolfram, A. Xagorari, P. Xander, J. Xu, X. Yan, M. Yáñez-Mó, H. Yin, Y. Yuana, V. Zappulli, J. Zarubova, V. Žėkas, J. Zhang, Z. Zhao, L. Zheng, A.R. Zheutlin, A.M. Zickler, P. Zimmermann, A.M. Zivkovic, D. Zocco, E.K. Zuba-Surma, Minimal information for studies of extracellular vesicles 2018 (MISEV2018): a position statement of the International Society for Extracellular Vesicles and update of the MISEV2014 guidelines, J. Extracell. Vesicles. 7 (2018) 1535750. doi:10.1080/20013078.2018.1535750.

[15] A. Morales-Kastresana, B. Telford, T.A. Musich, K. McKinnon, C. Clayborne, Z. Braig, A. Rosner, T. Demberg, D.C. Watson, T.S. Karpova, G.J. Freeman, R.H. Dekruyff, G.N. Pavlakis, M. Terabe, M. Robert-Guroff, J.A. Berzofsky, J.C.

Jones, Labeling extracellular vesicles for nanoscale flow cytometry, Sci. Rep. 7 (2017) 1878. doi:10.1038/s41598-017-01731-2.

[16] S. Gholizadeh, M. Shehata Draz, M. Zarghooni, A. Sanati-Nezhad, S. Ghavami, H. Shafiee, M. Akbari, Microfluidic approaches for isolation, detection, and characterization of extracellular vesicles: Current status and future directions, Biosens. Bioelectron. 91 (2017) 588–605. doi:10.1016/j.bios.2016.12.062.

[17] K. Boriachek, M.K. Masud, C. Palma, H.P. Phan, Y. Yamauchi, M.S.A. Hossain, N.T. Nguyen, C. Salomon, M.J.A. Shiddiky, Avoiding pre-isolation step in exosome analysis: Direct isolation and sensitive detection of exosomes using gold-loaded nanoporous ferric oxide nanozymes, Anal. Chem. 91 (2019) 3827–3834. doi:10.1021/acs.analchem.8b03619.

[18] B.A. Brown, X. Zeng, A.R. Todd, L.F. Barnes, J.M.A. Winstone, J.C. Trinidad, M. V. Novotny, M.F. Jarrold, D.E. Clemmer, Charge detection mass spectrometry measurements of exosomes and other extracellular particles enriched from bovine milk, Anal. Chem. 92 (2020) 3285–3292. doi:10.1021/acs.analchem.9b05173.

[19] A.S. Lawrie, A. Albanyan, R.A. Cardigan, I.J. MacKie, P. Harrison, Microparticle sizing by dynamic light scattering in fresh-frozen plasma, Vox Sang. 96 (2009) 206–212. doi:10.1111/j.1423-0410.2008.01151.x.

[20] C. Gardiner, Y.J. Ferreira, R.A. Dragovic, C.W.G. Redman, I.L. Sargent, Extracellular vesicle sizing and enumeration by nanoparticle tracking analysis, J. Extracell. Vesicles. 2 (2013) 19671. doi:10.3402/jev.v2i0.19671.

[21] P. Cizmar, Y. Yuana, Detection and characterization of extracellular vesicles by transmission and cryo-transmission electron microscopy, in: W.P. Kuo, S. Jia (Eds.), Extracellular Vesicles. Methods in Molecular Biology, 1st ed., Springer

Science+Business Media, 2017: pp. 221–232. doi:10.1007/978-1-4939-7253-1_18.

[22] J. Stetefeld, S.A. McKenna, T.R. Patel, Dynamic light scattering: a practical guide and applications in biomedical sciences, Biophys. Rev. 8 (2016) 409–427. doi:10.1007/s12551-016-0218-6.

[23] S. Bhattacharjee, DLS and zeta potential - What they are and what they are not?, J. Control. Release. 235 (2016) 337–351. doi:10.1016/j.jconrel.2016.06.017.

[24] S.P. Radko, A. Chrambach, Separation and characterization of sub-μm- and μm-sized particles by capillary zone electrophoresis, Electrophoresis. 23 (2002) 1957–1972. doi:10.1002/1522-2683(200207)23:13<1957::AID-ELPS1957>3.0.CO;2-I.

[25] S. Dziomba, K. Ciura, P. Kocialkowska, A. Prahl, B. Wielgomas, Gold nanoparticles dispersion stability under dynamic coating conditions in capillary zone electrophoresis, J. Chromatogr. A. 1550 (2018) 63–67. doi:10.1016/j.chroma.2018.03.038.

[26] K.R. Riley, S. Liu, G. Yu, K. Libby, R. Cubicciotti, C.L. Colyer, Using capillary electrophoresis to characterize polymeric particles, J. Chromatogr. A. 1463 (2016) 169–175. doi:10.1016/j.chroma.2016.08.017.

[27] X. Song, L. Li, H. Qian, N. Fang, J. Ren, Highly efficient size separation of CdTe quantum dots by capillary gel electrophoresis using polymer solution as sieving medium, Electrophoresis. 27 (2006) 1341–1346. doi:10.1002/elps.200500428.

[28] U. Franzen, J. Østergaard, Physico-chemical characterization of liposomes and drug substance-liposome interactions in pharmaceutics using capillary electrophoresis and electrokinetic chromatography, J. Chromatogr. A. 1267 (2012) 32–44. doi:10.1016/j.chroma.2012.07.018.

[29] L. Kremser, G. Bilek, D. Blaas, E. Kenndler, Capillary electrophoresis of viruses, subviral particles and virus complexes, J. Sep. Sci. 30 (2007) 1704–1713. doi:10.1002/jssc.200700105.

[30] E. van Tricht, L. Geurink, H. Backus, M. Germano, G.W. Somsen, C.E. Sänger–van de Griend, One single, fast and robust capillary electrophoresis method for the direct quantification of intact adenovirus particles in upstream and downstream processing samples, Talanta. 166 (2017) 8–14. doi:10.1016/j.talanta.2017.01.013.

[31] P.B. Allen, B.R. Doepker, D.T. Chiu, High-throughput capillary-electrophoresis analysis of the contents of a single mitochondria, Anal. Chem. 81 (2009) 3784–3791. doi:10.1021/ac900099y.

[32] M. Piotrowska, K. Ciura, M. Zalewska, M. Dawid, B. Correia, P. Sawicka, B. Lewczuk, J. Kasprzyk, L. Sola, W. Piekoszewski, B. Wielgomas, K. Waleron, S. Dziomba, Capillary zone electrophoresis of bacterial extracellular vesicles: A proof of concept, J. Chromatogr. A. 1621 (2020) 461047. doi:10.1016/j.chroma.2020.461047.

[33] M. Morani, T.D. Mai, Z. Krupova, P. Defrenaix, E. Multia, M.L. Riekkola, M. Taverna, Electrokinetic characterization of extracellular vesicles with capillary electrophoresis: A new tool for their identification and quantification, Anal. Chim. Acta. 1128 (2020) 42–51. doi:10.1016/j.aca.2020.06.073.

[34] U. Nobbmann, Derived count rate – what is it?, Malvern Panalytical - Mater. Talks. (2015). https://www.materials-talks.com/blog/2015/06/11/derived-count-rate-what-is-it/ (accessed October 6, 2020).

[35] A. Guttman, A.S. Cohen, D.N. Heiger, B.L. Karger, Analytical and micropreparative ultrahigh resolution of oligonucleotides by polyacrylamide gel

high-performance capillary electrophoresis, Anal. Chem. 62 (1990) 137–141. doi:10.1021/ac00201a010.

[36] A.E. Barron, W.M. Sunada, H.W. Blanch, The effects of polymer properties on DNA separations by capillary electrophoresis in uncross-linked polymer solutions, Electrophoresis. 17 (1996) 744–757. doi:10.1002/elps.1150170421.

[37] D. Heiger, High-performance capillary electrophoresis, 1st Ed., Agilent Technologies, Germany, 2000. doi:10.1039/9781847550521-00208.

[38] M.C. Deregibus, F. Figliolini, S. D'Antico, P.M. Manzini, C. Pasquino, M. De Lena, C. Tetta, M.F. Brizzi, G. Camussi, Charge-based precipitation of extracellular vesicles, Int. J. Mol. Med. 38 (2016) 1359–1366. doi:10.3892/ijmm.2016.2759.

[39] S.L. Tamisier-Karolak, S. Pagliarusco, C. Herrenknecht, M. Brettreich, A. Hirsch, R. Céolin, R. V. Bensasson, H. Szwarc, F. Moussa, Electrophoretic behavior of a highly water-soluble dendro[60]fullerene, Electrophoresis. 22 (2001) 4341–4346. doi:10.1002/1522-2683(200112)22:20<4341::AID-ELPS4341>3.0.CO;2-I.

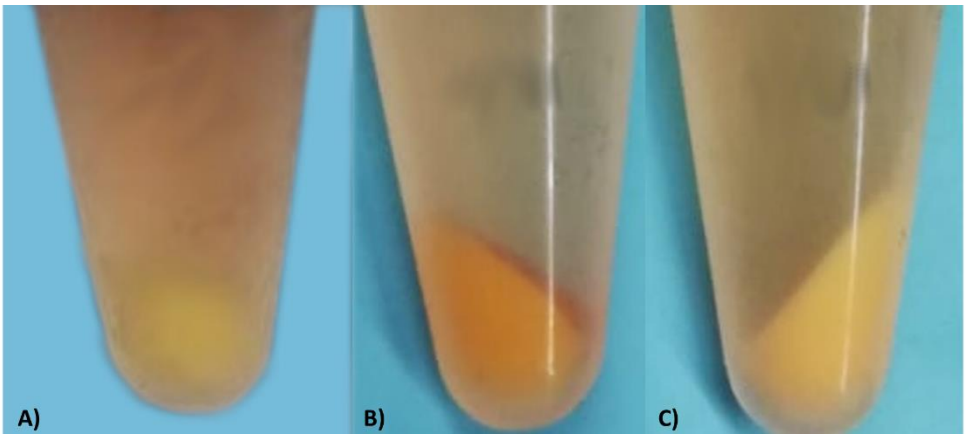

Figure 1. EV preparations isolated from serum using A) 5, B) 7.5 and C) 10% m/v of PEG (4 °C and 2 h incubation).

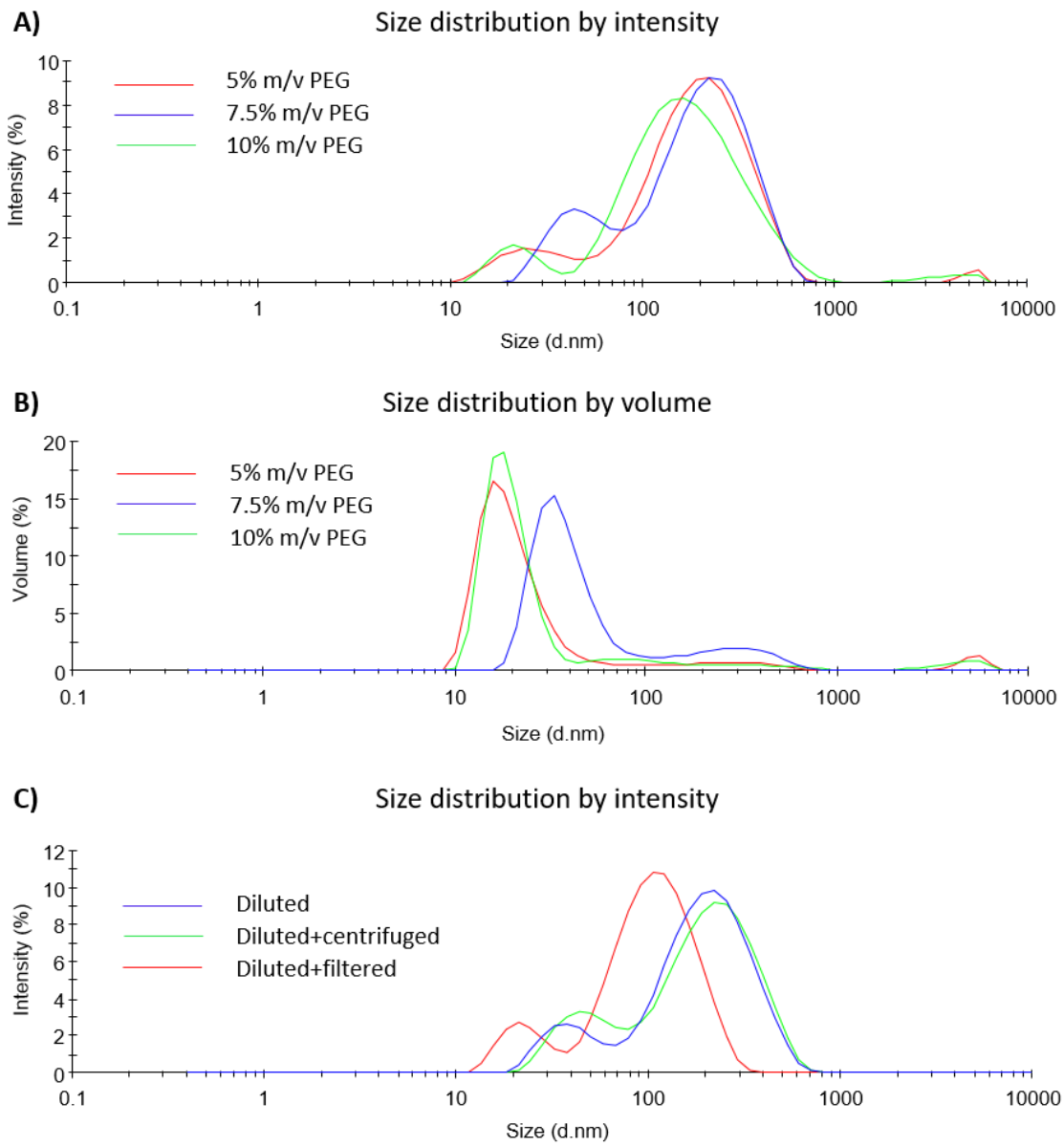

Figure 2. Size distribution of the particles of the EV preparations by DLS (samples were diluted 1:10 v/v with PBS). Graph of size distribution by A) intensity with different PEG concentrations, B) graph of size distribution by volume with different PEG concentrations and C) graph of size distribution by intensity with 10% m/v PEG for the samples "diluted", "diluted+filtered" (0.2 µm nylon filters) and "diluted+centrifuged" (1,250 x g for 3 min at 25 ºC).

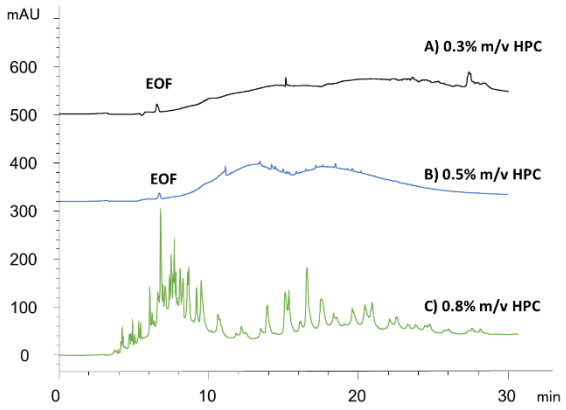

Figure 3. Electropherograms for the EV preparations isolated with 10% m/v PEG using the BGE of 0.1 M Tris and 0.25 M boric acid (pH 7.9) with A) 0.3, B) 0.5 and C) 0.8% m/v of HPC. Detection wavelength was 210 nm. A neutral marker solution (5% v/v acetone) was analyzed to confirm the EOF migration time.

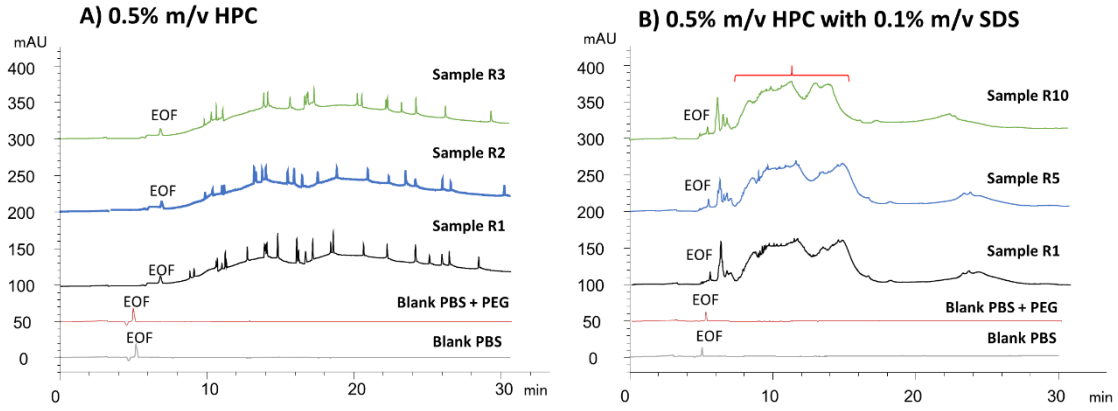

Figure 4. Electropherograms for the EV preparations isolated with 10% m/v PEG using the BGE of 0.1 M Tris and 0.25 M boric acid (pH 7.9) with A) 0.5% m/v HPC (n=3) and B) 0.5% m/v HPC and 0.1% m/v SDS (n=10, replicates 1st, 5th and 10th). Detection wavelength was 210 nm. A neutral marker solution (5% v/v acetone) was analyzed to confirm the EOF migration time. Blank samples were 10% m/v PEG in water or PBS. The marked central band was integrated for migration time and peak area repeatability calculations.

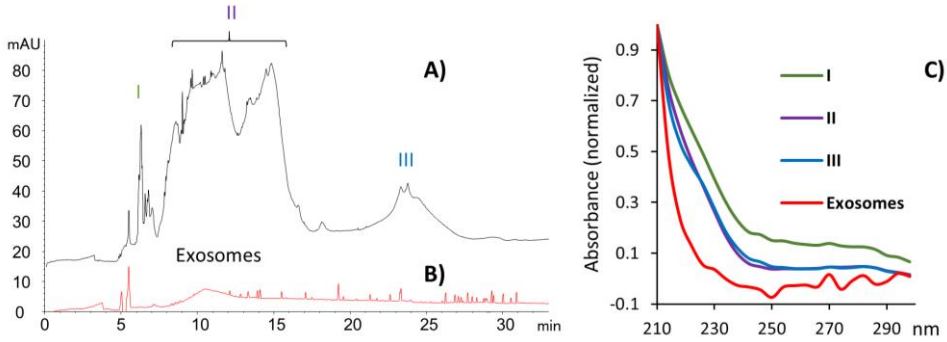

Figure 5: Electropherograms under the optimized conditions for A) the EV preparations and B) the standard exosomes. C) UV-spectra for the groups of peaks and bands labelled as I, II and III in the electropherogram of the EV preparation (Figure 5A) and for the exosomes (Figure 5B) (the absorbance y-scale was normalized to the maximum absorbance in each case: 21.5, 46.5, 14.5 and 3.0 mAU for I, II, III and the exosomes. The quality of the normalized UV spectrum for the exosomes was poor over 250 nm due to the very low absorbance of the raw data).

Table 1. Size distribution of the particles of the EV preparations by DLS (graph of size distribution by intensity, Figure 2A) with different PEG concentrations and sample conditions. Samples were diluted with PBS ("diluted"), followed by centrifugation ("diluted+centrifuged") or by filtration ("diluted+filtered").

% m/v PEG	Sample conditions	PDI	Z-average[a] (nm)	Peaks[b]	Average size (nm)	Standard deviation (nm)	Intensity (%)
10	Diluted	0.432	122	Peak 1	242	114	79
				Peak 2	50	16	21
	Diluted+centrifuged	0.435	125	Peak 1	227	108	84
				Peak 2	42	13	16
	Diluted+filtered	0.298	74	Peak 1	119	52	86
				Peak 2	27	7	14
7.5	Diluted	0.439	116	Peak 1	204	134	90
				Peak 2	23	6	8
5	Diluted	0.489	126	Peak 1	223	117	88
				Peak 2	29	11	11

[a] The Z-average size is given as a complementary information considering a moderately monodisperse and monomodal sample.
[b] See Figure 2A.

Table 2. Derived count rate (DCR) values of the particles of the EV preparations by DLS with different PEG concentrations and sample conditions. Samples were diluted with PBS ("diluted"), followed by centrifugation ("diluted+centrifuged") or by filtration ("diluted+filtered).

% m/v PEG	Sample conditions	DCR (kcps)
10	Diluted	53414
	Diluted+centrifuged	50649
	Diluted+filtered	3654
7.5	Diluted	50580
	Diluted+centrifuged	47674
	Diluted+filtered	8161
5	Diluted	6908
	Diluted+centrifuged	7083
	Diluted+filtered	415

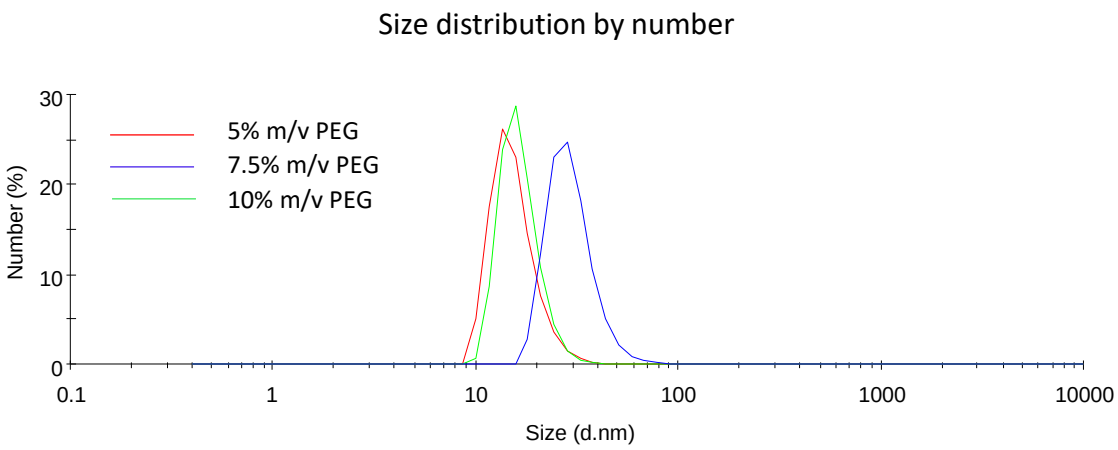

Figure S-1. (Size distribution of the particles of the EV preparations by DLS (samples were diluted 1:10 v/v with PBS). A) Graph of size-distribution by number with different PEG concentrations.

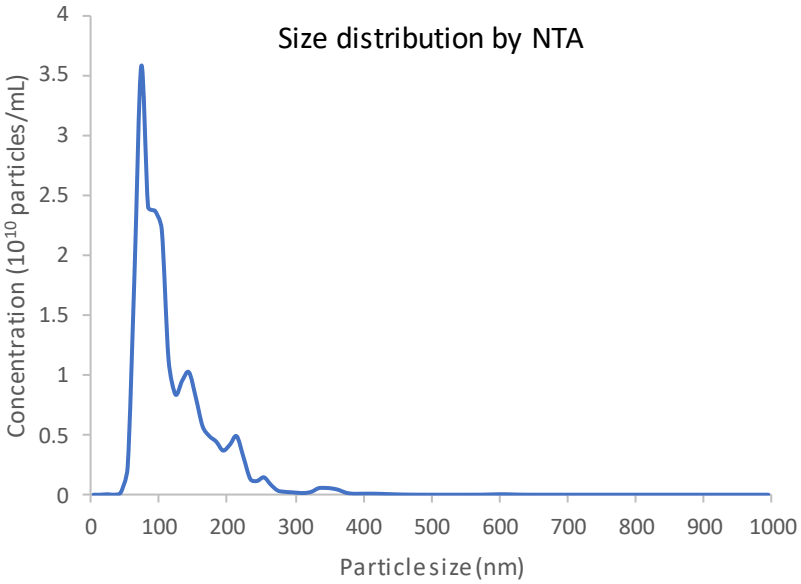

Figure S-2. Size distribution of the particles of the EV preparation isolated with 10% m/v PEG by NTA (samples were diluted 1:500 v/v with PBS). Measured average particle size was 120 nm.

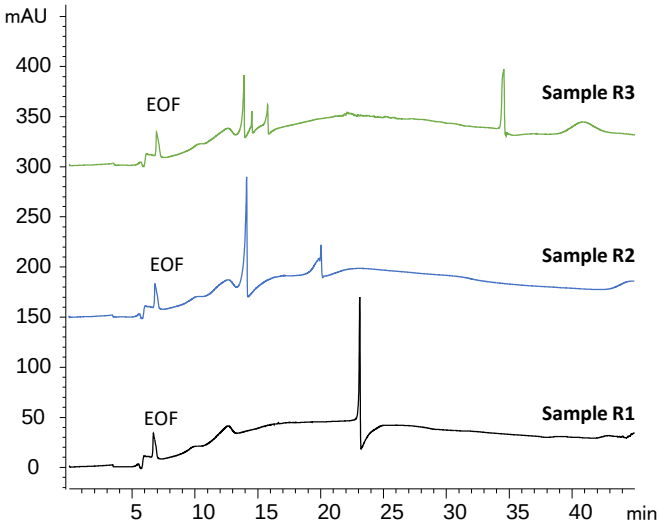

Figure S-3. Electropherograms for three replicate analyses of the EV preparation isolated with 10% m/v PEG using the BGE of 0.1 M Tris and 0.25 M boric acid (pH 7.9). A neutral marker solution (5% v/v acetone) was analyzed to confirm the EOF migration time.

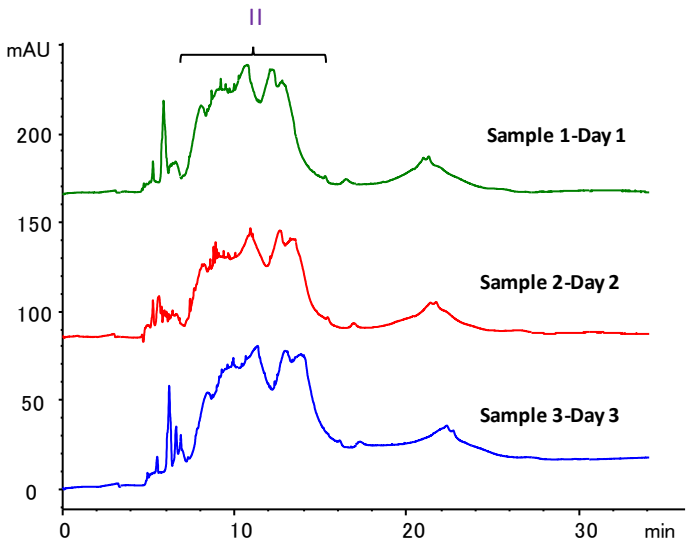

Figure S-4. Electropherograms for three independent EV preparations isolated with 10% m/v PEG and analyzed in different days using the BGE of 0.1 M Tris and 0.25 M boric acid (pH 7.9) with 0.5% m/v HPC and 0.1% m/v SDS. Detection wavelength was 210 nm. The marked central band (region II) was integrated for migration time and peak area reproducibility calculations.